



UNIVERSITY
of
GLASGOW

Department of Physics & Astronomy
Experimental Particle Physics Group

Kelvin Building, University of Glasgow,

Glasgow, G12 8QQ, Scotland

Telephone: +44 (0)141 339 8855 Fax: +44 (0)141 330 5881

GLAS-PPE/97-02

10th September 2018

QCD Effects in Hadronic Final States

E. A. De Wolf (Universitaire Instelling Antwerpen), A. T. Doyle (University of Glasgow),
N. Varelas (Michigan State University) and D. Zeppenfeld (University of Wisconsin).

*Summary of the Hadronic Final States Working Group
at the DIS97 Workshop, Chicago (April 1997).*

Abstract

Progress in the study of hadronic final states in deep inelastic scattering as well as $p\bar{p}$, photoproduction and e^+e^- annihilation, as presented at the DIS97 workshop, is reviewed.

Introduction

The large centre of mass energies and increasing statistical precision available at HERA, the Tevatron and LEP combined with recent theoretical developments open a new testing ground for QCD. The presentations on hadronic final states presented at the DIS97 workshop place increasingly significant experimental and theoretical constraints on the strong interaction. This summary focuses on the common themes and highlights of the hadronic final states working group.

arXiv:hep-ex/9707038v1 26 Jul 1997

Fragmentation

Perturbative QCD (pQCD) has proved to be a very successful theory in its application to hard processes. This enables the theory to be employed as a tool to tackle more complicated problems. One of these concerns the soft limit of QCD and colour confinement. Presently, multihadron production phenomena cannot be derived in a systematic way solely from perturbation theory without additional model-dependent assumptions.

To investigate the limits of applicability of pQCD it is important to determine to what extent semi-soft phenomena in hard processes still reflect the properties of the perturbative evolution phase. This line of research, initiated almost 15 years ago [1,2], has reached a high level of sophistication (see [3] for a recent review) and, as witnessed at this workshop, continues to inspire analyses in all major high-energy experiments. This summary deals with some of the most interesting results.

Particle Rates

In the current picture of hadron production, factorisation plays a predominant role in the different evolution stages of the process: ‘preparation’ of the primary partonic configuration, additional parton production described e.g. by (angular-ordered) parton showers (pQCD), hadron formation described e.g. by string or cluster fragmentation (non-perturbative QCD), secondary hadronic cascade-decays (QFD and non-perturbative QCD). To test such an ansatz, a comparative study of jet properties—including particle rates and spectra—in different reactions is required. At present this has not yet become a topic of primary interest at hadron-hadron colliders and HERA in spite of its importance for QCD.

How much remains to be done is illustrated in [4] where the impressive results from the LEP experiments are updated and reviewed. As far as hadron production is concerned, 38 different inclusive production rates of mesons and baryons are now measured at the Z^0 and, for many of these, inclusive spectra are available.

In all, good agreement is observed for the rates with tuned versions of JETSET 7.4 [5] and HERWIG 5.9 [6]. A noteworthy exception is the baryon sector which remains an embarrassment for HERWIG. Either a better retuning or a critical re-evaluation of the cluster decay model seems required. The Lund JETSET string approach fares better but contains a large number of parameters related to flavour and spin. Since this number is increasing with time, little real predictive power is left.

In e^+e^- annihilation at LEP, evidence for breaking of ‘jet universality’ and factorisation may have been found from excess η production—above JETSET expectations—at large momentum in three-jet events [7] (glueball production or surplus iso-singlet hadrons?) while no anomaly is seen for π^0 production. It could be that the long-awaited direct manifestation of gluon jet fragmentation has finally been found [8]. If so, even larger discrepancies could be expected for the η' [9]. The $f_0(975)$ and $a_0(980)$ mesons could also play a special role in the dynamics of quark confinement [10]. A comparative study of these and other hadrons in quark and in gluon jets is called for.

Problems also appear with strangeness production (mainly K and Λ) where DELPHI notes a deficit of strange particles in extreme two-jet events [11]: the production of strangeness depends on the *event topology* in a manner that is not quantitatively described by JETSET.

Although HERA experiments have only started to investigate the field so thoroughly explored at LEP, and information on *identified* particles is still scarce, first evidence has been found that the level of strangeness production in DIS and photoproduction, translated into a s/u relative production rate is close to 0.2, to be compared with 0.3 in e^+e^- [12].

Lessons to be learned from the vast amount of data in e^+e^- annihilations at the Z^0 are that deviations from ‘universal fragmentation’ may well have been observed and that the topology of the confining QCD fields is likely to play a role in hadroproduction. The rich variety of such topological configurations possible in ep collisions poses a real challenge for the experimentalists.

Particle Spectra

A striking prediction of the perturbative approach to QCD jet physics is the depletion of soft particle production and the resulting approximately Gaussian shape of the inclusive distribution in the variable $\xi = \log E_{jet}/E$ for particles with energy E in a jet of energy E_{jet} —the famous “hump-back plateau” [2]. Due to the *intrajet* coherence of gluon radiation, not the softest partons but those with intermediate energies ($E \propto E_{jet}^{0.3-0.4}$) multiply most effectively in QCD cascades.

The shapes of the measured particle energy spectra in e^+e^- annihilation turn out to be surprisingly close, over the whole momentum range down to momenta of a few hundred MeV, to the perturbative predictions based on the Modified Leading Log Approximation (MLLA) [3]. These observations can be taken as evidence that the perturbative phase of the cascade development indeed leaves its imprint on the final state hadrons. This, in turn, suggests that the conversion of partons into hadrons occurs at a low virtuality scale (of the order of the hadron masses), independent of the scale of the primary process, and involves only low-momentum transfers. This Local Parton-Hadron Duality (LPHD) may be connected to pre-confinement properties of QCD which ensure that colour charges are compensated locally [13]. LPHD remains, however, a strong hypothesis that is supposed to be valid only in an inclusive and average sense. With LPHD, only two essential parameters are involved in the perturbative description: the effective QCD scale Λ and a (transverse momentum) cut-off parameter Q_0 , resulting in a highly constrained theoretical framework; non-perturbative effects are essentially reduced to normalisation constants.

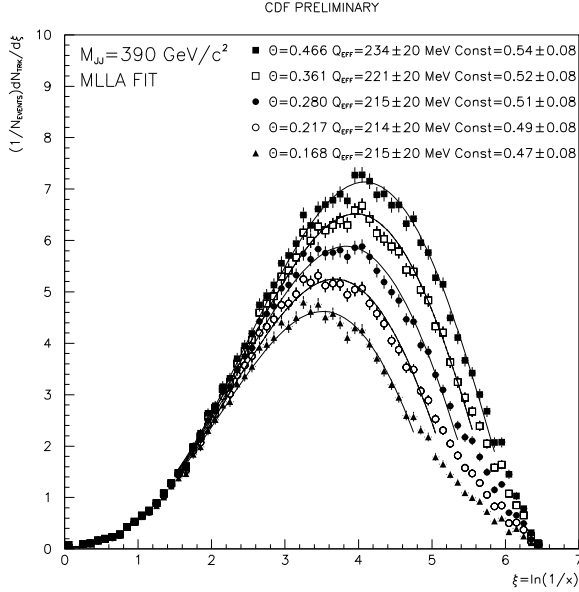
New data on charged particle spectra were presented at this workshop by H1 [14], ZEUS [15] and CDF [16]. The HERA experiments concentrate on the current fragmentation region in DIS and perform the analysis in the Breit frame, where the exchanged boson is completely spacelike. The new data confirm with much increased statistical significance the features observed in e^+e^- : approximately Gaussian shape of the ξ spectra with peak-position and width increasing with Q as predicted in MLLA. Moreover, for sufficiently large Q , they demonstrate the expected equivalence of the current region with one hemisphere of an e^+e^- event. With increasing luminosity being accumulated at HERA, this work should be extended to include moment and cumulant analyses of the spectra for which detailed predictions exist [3].

Beautiful confirmation of the MLLA+LPHD approach has been presented by CDF [16]. This experiment studies charged particle momentum distributions in subsamples of dijet events. For fixed dijet masses (hence fixed jet energy) in the range $83 < M_{JJ} < 625$ GeV, the ξ distribution of tracks, within cones of various opening angle Θ (with respect to the jet axis), is studied (see Fig. 1(a)). As dijet mass \times jet opening angle increases, the peak of the spectrum, ξ_0 , shifts towards larger values of ξ in perfect agreement with MLLA predictions and e^+e^- data, as shown in Fig. 1(b). Similar analyses should be possible in DIS and photoproduction at HERA but have not yet been attempted.

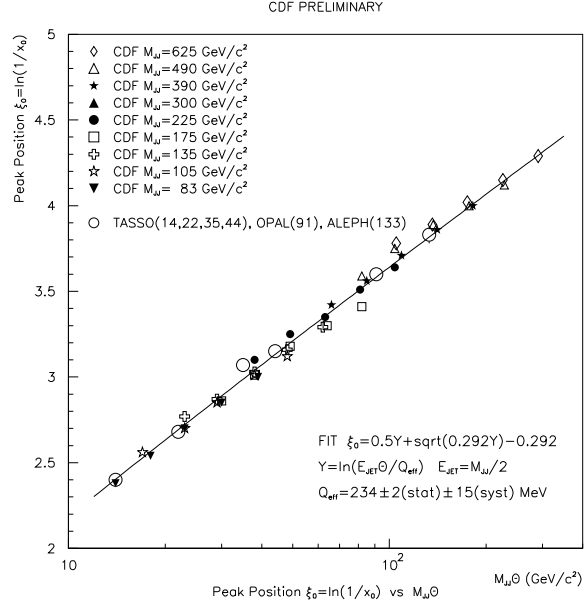
Although present data on charged particles appear to confirm strikingly the perturbative approach to soft hadronisation, the situation is less clear-cut when spectra of identified particles/resonances are examined. At LEP, the conclusion is unambiguous: the peak positions do not agree with the naively expected mass dependence. Here also, data on spectra of different hadron species and from different jets at the Tevatron and HERA would be most helpful.

Limiting behaviour at low momenta

The analytical perturbative approach allows one to predict the limit of the one-particle invariant density in QCD jets $Edn/d^3p \equiv dn/dy d^2p_T$ at very small momenta p or, equivalently, in the limit of vanishing rapidity and transverse momentum [17]. If the dual description of hadronic and partonic states is adequate down to very small momenta, a finite, energy-independent limit of the invariant hadronic density, I_0 , is expected. This is a direct consequence of the colour coherence in soft gluon branching. A possible rise of I_0 with centre-of-mass energy would indicate that either coherence or the local duality (or both) break down. Since colour coherence is a general property of QCD as a gauge theory, it is the LPHD concept that is tested in measurements of the soft hadrons.



(a) Evolution of ξ with jet opening angle, Θ , for $M_{JJ} = 390$ GeV.



(b) Evolution of the peak position with $M_{JJ}\Theta$.

Figure 1: Comparison of preliminary CDF inclusive momentum distributions with MLLA predictions and e^+e^- annihilation data.

The e^+e^- annihilation data on charged and identified particle inclusive spectra have been found to follow the MLLA prediction surprisingly well, also at low centre-of-mass energies. The invariant spectra at low momentum scale approximately (within 10%) between 1.6 and 140 GeV and agree with perturbative calculations which become very sensitive to the strong running of α_S at small scales [18].

At this workshop, H1 presented the first Breit frame measurements of the invariant energy spectra in DIS as a function of Q , (see Fig. 3 in [14]). For sufficiently high Q , the data show that the low-momentum limit in that region of phase space is essentially independent of Q and indeed similar to that in e^+e^- annihilation.

Scaling violations

Whereas the preceding paragraphs dealt mainly with the semi-soft limit of the hadron spectra, promising results from H1 and ZEUS were presented to this workshop on the scaling violations at larger values of the scaled momentum $x_p = 2p/Q$ [14,15]. In QCD, scaling violations of the fragmentation function are expected, in full analogy with scaling violations of structure functions, due to increased gluon radiation. This leads to softer particle spectra with increasing energy. In principle, the scaling violations at large x_p allow a measurement of α_S and have been exploited for that purpose in e^+e^- annihilation. Whereas different e^+e^- experiments must be combined to cover a sufficient range in centre-of-mass energy, this can be accomplished for ep collisions in a single experiment.

H1 data provides evidence for violation of scaling in the current region of the Breit frame. The corresponding ZEUS data, shown in Fig. 2, have also been compared with the CYCLOPS NLO calculation [19] incorporating fragmentation functions taken from e^+e^- [15]. The data at large x_p show a weak dependence on the input proton parton densities but a clear sensitivity to α_S . With analysis of more, already existing, data it should become possible to use the complete NLO calculations to extract α_S in DIS.

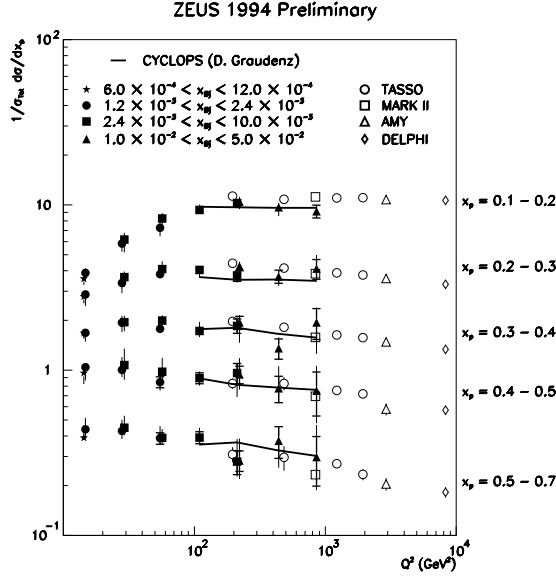


Figure 2: $1/\sigma_m d\sigma/dx_p$ measurement as a function of Q^2 . The preliminary ZEUS data are compared to data from e^+e^- annihilation experiments and the CYCLOPS NLO calculation of the inclusive charged hadron spectra.

Multiple Interactions

At this workshop, CDF presented preliminary results on the measurement of events where two scattering processes occur in the same event [20]. For distinct processes A and B , the cross section for this “double parton (DP) scattering” is given by $\sigma_{DP} = \sigma_A \sigma_B / \sigma_{\text{eff}}$, where σ_{eff} is a process independent parameter.

Events were selected with a relatively low transverse energy ($E_T > 16$ GeV) “photon” trigger in conjunction with three jets with $E_T > 5$ GeV. The separation of DP events from the underlying QCD background is determined by studying variables sensitive to decorrelation effects. In particular, the azimuthal angle between the two best-balancing pairs (“photon”+jet versus dijet) is approximately flat for the DP signal and enables a statistical separation of events. A new feature of this analysis is that events with displaced vertices, where the jets are reconstructed from separate origins, are used to evaluate $\sigma_A \sigma_B$ directly and hence reduce the theoretical uncertainties. This allows the first relatively precise determination of the effective cross section:

$$\sigma_{\text{eff}} = (14.5 \pm 1.7_{-2.3}^{+1.7}) \text{ mb.}$$

No x -dependence is observed, within the uncertainty of $\simeq 20\%$. Assuming a uniformly dense ball of partons and using the measured inelastic $p\bar{p}$ cross section, one expects $\sigma_{\text{eff}} = 11$ mb. The measurement represents a milestone in the study of multiple interactions and provides the first significant experimental constraint on such processes.

Multiple interactions, where two or more partons interact in the same event, represent a considerable uncertainty in the analysis of photoproduction events at HERA. In particular, the extraction of the gluon content of the photon at relatively low x_γ requires careful modelling of these interactions, since they can contribute up to 50% of the cross section at the relatively low E_T values ($E_T > 6$ GeV) measured so far. The Tevatron result should aid in a realistic estimate of the uncertainties due to multiple interactions in the extraction of the gluon density of the photon at HERA. Similarly, such measurements improve background estimates to di-boson and boson+jet production at the Tevatron as well as the predictions of jet rates from multiple interactions at the LHC.

Event Shapes

The measurement of event shape variables has been well-established in e^+e^- annihilation experiments. An important point in the development of our understanding of QCD is to ensure that the measurement is well-defined theoretically at the required level of precision. In this case variables are chosen which are relatively insensitive to soft gluon emission and collinear parton branching. A determination of $\alpha_S(\mu)$ is therefore possible by comparison with NLO theory plus resummed series or NLLA calculations. At this workshop, impressive results from LEP II were presented which enabled a LEP average $\alpha_S(M_Z) = 0.120 \pm 0.005$ to be extracted [21].

Recent theoretical developments in the understanding of infrared renormalon contributions, which lead to divergences from the perturbative calculations, allow the first steps to be made towards a direct comparison of theory and data without invoking hadronisation models. These power corrections, with a characteristic $1/Q$ dependence, have been calculated for event shape variables [22] and could also be calculated for differential jet rates.

H1 presented new measurements of the thrust, jet broadening and jet mass in DIS for momentum transfers, $7 < Q < 100$ GeV, in the current region of the Breit frame [23]. The mean values of the event shape data show similar trends to results from e^+e^- annihilation experiments as a function of Q . In the DIS case, one advantage is that the event axis is determined by the direction of the virtual boson, whereas in e^+e^- annihilation the axis has to be determined from the final state hadrons using e.g. the thrust axis. The data, shown in Fig. 3, have been fitted to NLO theory plus the calculated power corrections of Dasgupta and Webber. The important conclusion is that the size of the power correction, characterised by the parameter $\bar{\alpha}_o$, is consistent with a single value of $\bar{\alpha}_o = 0.491 \pm 0.003$ (exp) $^{+0.079}_{-0.042}$ (theory) for three of the four event shape variables. In the case of jet broadening, the calculation of the power corrections is subject to large uncertainties: hence this particular variable does not satisfy the requirement of being theoretically well-defined and is not included in the global fit. The development of these power corrections is not only intrinsically important, but should also enable more precise extractions of α_S by constraining the hadronisation uncertainties more precisely.

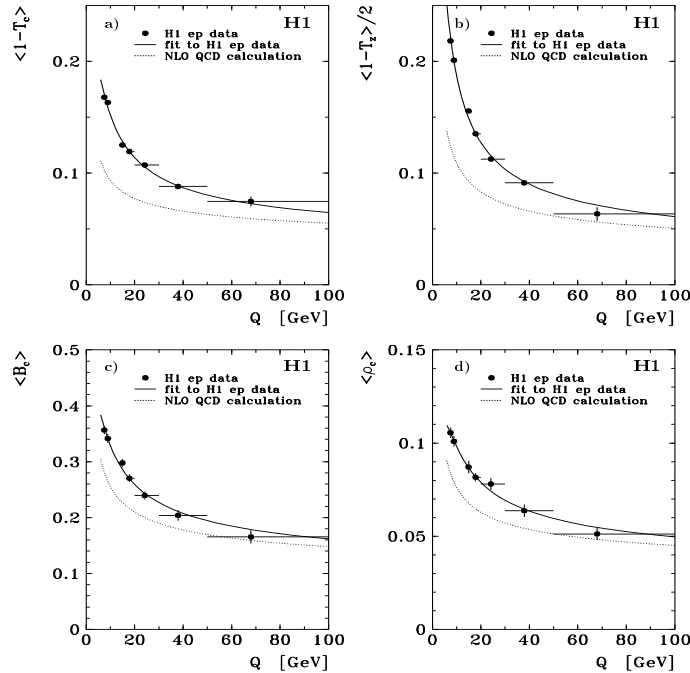


Figure 3: Mean values of event shape variables as a function of Q , from H1. The values are for 1-thrust, calculated using (a) the thrust axis or (b) the photon axis, (c) the jet broadening and (d) the jet mass. The dotted line indicates the NLO calculation. The full line indicates the fit incorporating power corrections.

Jet Shapes

The shape of the transverse energy distribution of particles within a jet produced in various interactions allows the primary parton source of the jet to be identified. In addition, the data provide strong constraints on the coherence properties of the showering partons and enable tests of the universality of the fragmentation process. In an analysis from the ZEUS Collaboration [24], the jet shapes measured in photoproduction and DIS were compared with those from e^+e^- annihilation and $p\bar{p}$ experiments. Jets are measured using the cone algorithm with a cone radius of 1. The jet shape, $\psi(r)$, is defined as the average fraction of the jet's transverse energy that lies within an inner cone of radius r . The distributions shown in Fig. 4 are therefore integral plots with $\psi(r)=1$ at $r=1$, whose rate of fall-off measures how broad the jet is. The data shown are for minimum jet transverse energies around 40 GeV. It is observed that the DIS and e^+e^- data contain $\simeq 70\%$ of their transverse energy within a sub-cone radius of 0.2, consistent with well-collimated quark jets. In contrast, the $p\bar{p}$ data jets are rather broad, with only $\simeq 50\%$ of their transverse energy being contained within the same sub-cone radius, consistent with predominantly gluon jets in this E_T range.

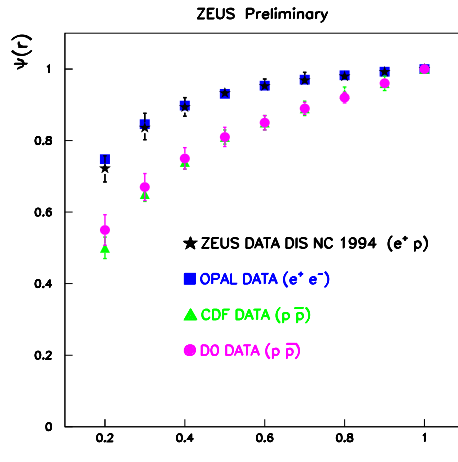


Figure 4: Comparison of jet shape measurements from ZEUS(DIS), OPAL(e^+e^-), CDF and DØ ($p\bar{p}$). The jet energy ranges are $37 < E_T^{\text{jet}} < 45$ GeV, $35 \text{ GeV} < E_T^{\text{jet}}$, $40 < E_T^{\text{jet}} < 60$ GeV and $45 < E_T^{\text{jet}} < 70$ GeV, respectively.

Photoproduction data (see Fig. 2 in [24]) were also studied as a function of pseudorapidity and transverse energy. The observed changes in jet shape were reproduced in models which incorporate both direct and resolved photon processes provided that the resolved processes include the multiple interactions discussed above. NLO calculations from Klasen and Kramer [25] determine the jet shape only at the lowest non-trivial order. In order to describe the data, an R_{sep} parameter is introduced which determines when two partons are merged into a single jet. The jet shape distribution is well described by NLO calculations with an R_{sep} parameter which increases with increasing rapidity in the proton direction, but which is in the range $1.3 < R_{\text{sep}} < 1.8$. Differential distributions of the average transverse energy in intervals of cone radius will enable R_{sep} to be fitted and provide further constraints on the models.

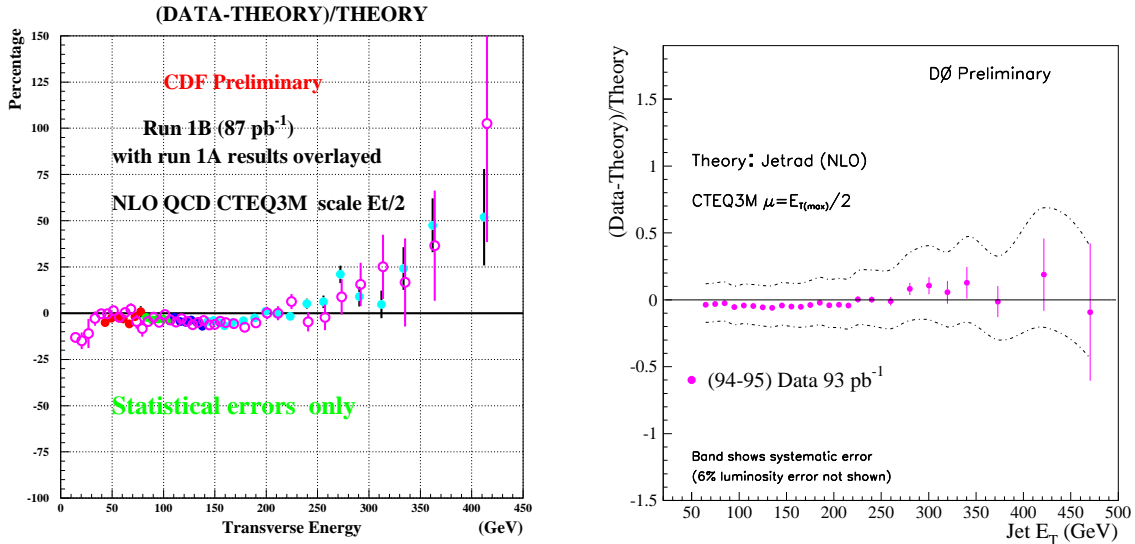
High- E_T Jet Results from the Tevatron

The Tevatron Collider provides a unique opportunity to study the properties of hard interactions in $p\bar{p}$ collisions at short distances. The production of jets at large E_T and its comparison with perturbative QCD calculations are of interest as they can serve as a test of the elementarity of the partons.

The CDF and DØ collaborations have measured jet cross sections over ten orders of magnitude in $d^2\sigma/dE_T d\eta$ up to $E_T = 500$ GeV, half way to the kinematic limit. The challenge of measuring such a steeply falling

spectrum is the understanding of the energy calibration of jets. The highest E_T jets are not directly calibrated, resulting in large uncertainties. In this kinematic region the NLO calculations are well understood at the 10–20% level. However, precise knowledge of the parton distribution functions in the proton is required before firm conclusions can be drawn from the comparison of data and theory. Collider data can constrain the parton distribution functions in the proton and especially the gluon distribution at moderate x . Kosower presented a formalism to make such an extraction possible using NLO calculations, while minimising the amount of numerical computation involved [26].

The preliminary (published) inclusive jet cross sections as measured by CDF using the 1994–1995 (1992–1993) data sample in the pseudorapidity region of $0.1 \leq |\eta| \leq 0.7$ are compared to the NLO QCD in Fig. 5(a) [27,28]. The latter are based on calculations by EKS [29] with CTEQ3M [30] parton densities, renormalisation and factorisation scales $\mu = E_T^{\text{jet}}/2$, and the standard Snowmass jet cone algorithm. The data and the prediction are in excellent agreement for $E_T < 250$ GeV; at higher E_T , however, the data lie significantly above the predictions.



(a) CDF data vs. theory

(b) DØ data vs. theory

Figure 5: Ratio between experiment and theory for the inclusive jet cross section as measured by CDF and DØ.

DØ presented updated inclusive jet cross sections in the region of $|\eta| \leq 0.5$ with significantly reduced systematic uncertainties (by about a factor of two), coming from a re-evaluation of the jet energy scale corrections [27]. As shown in Fig. 5(b), these results are in excellent agreement with NLO QCD over the entire E_T range. DØ compares the data to NLO QCD predictions using JETRAD [31], the CTEQ3M parton densities, the renormalisation and factorisation scales $\mu = E_T^{\text{max}}/2$, and a modified Snowmass jet cone algorithm with $R_{\text{sep}}=1.3$.

It should be noted that the DØ and CDF data have been compared to NLO QCD with slightly different input parameters which can introduce an E_T -dependent variation of $\simeq 10\%$ on the theoretical predictions [27]. Also the two measurements probe different η regions.

In order to compare directly the results of the two experiments, DØ also performed the analysis in the CDF η region. Figure 6 shows the CDF data points as compared to a fit of the DØ data in the $0.1 \leq |\eta| \leq 0.7$ region. The error band corresponds to the DØ systematic error which is mainly due to the jet energy scale uncertainty. The CDF data lie above the DØ fit but are within the experimental uncertainties. For a more quantitative comparison between the two experiments, the correlations in the systematic uncertainties of the two data sets must be taken into account.

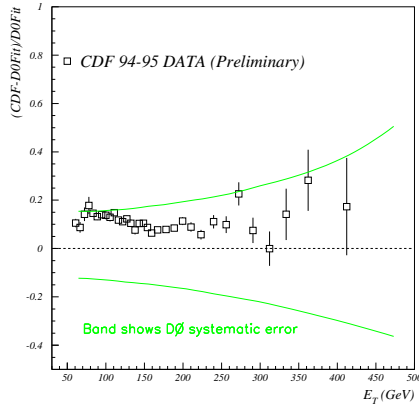


Figure 6: Residual plot of the CDF data with a fit on the $0.1 \leq |\eta| \leq 0.7$ $D\bar{D}$ data. The band shown represents the $D\bar{D}$ systematic uncertainty.

The dijet angular distribution is an ideal tool to determine whether any possible excess of events in high- E_T inclusive jet production is due to new physics effects. The angular distribution of the outgoing partons is strictly governed by the helicities of the partons participating in the hard process and is relatively insensitive to the parton densities. Any unusual contact interaction (with effective scale Λ) will flatten the centre of mass scattering angle distribution (or create an excess of events at low χ). The CDF published results on dijet angular distributions give a lower limit of $\Lambda > 1.8$ TeV. Figure 7 shows the recent $D\bar{D}$ χ distributions which are in good agreement with NLO QCD [27]. Using these data, $D\bar{D}$ rules out at 95% CL a model where quarks couple with a universal contact interaction of scale $\Lambda \sim 2.1$ TeV.

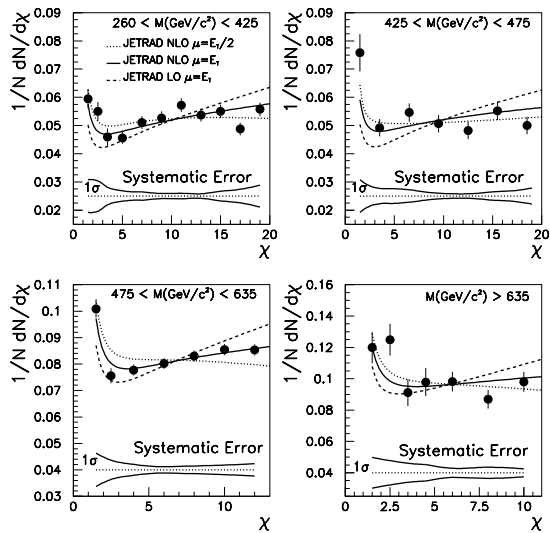


Figure 7: Dijet angular distributions for $D\bar{D}$ data compared to JETRAD for LO and NLO predictions with two different renormalisation/factorisation scales.

Dijet Production in DIS at HERA

A major area of study at HERA is dijet production in DIS, which has earlier been used to determine α_S and constrain the gluon density. Previously, data have been compared to NLO semi-analytic calculations using JADE-type algorithms. Now, with the flexible NLO Monte Carlo programs MEPJET [32] and DISENT [33] available, comparisons with various jet schemes are possible. Results were presented at this workshop using the cone [34,35], JADE [36] and k_T [37] algorithms.

In order to measure the cross sections, detailed comparisons with models incorporating parton showers/dipole chains and a hadronisation phase have been made. In general, these data are well described by the ARIADNE [38] program and are reasonably well described by LEPTO [39] or HERWIG [6]. The next stage in the development of ARIADNE by the Lund group is the Linked Dipole Chain (LDC) model, which was reported at this workshop [40].

A problem highlighted at the workshop relates to various attempts which have been made to correct to *parton* level in an attempt to determine the gluon density or the strong coupling constant directly. However, the relationship between the NLO partons and ARIADNE/LEPTO/HERWIG partons is far from clear and this introduces an uncertainty for theorists who wish to compare with published data. A presentation of the data corrected to hadron level is therefore required.

The general observation in various analyses, with a range of different kinematic cuts, is that the measured dijet cross sections/rates tend to be higher than those predicted by the NLO calculations incorporating a default coupling constant and parton densities which describe the total DIS cross sections¹⁾.

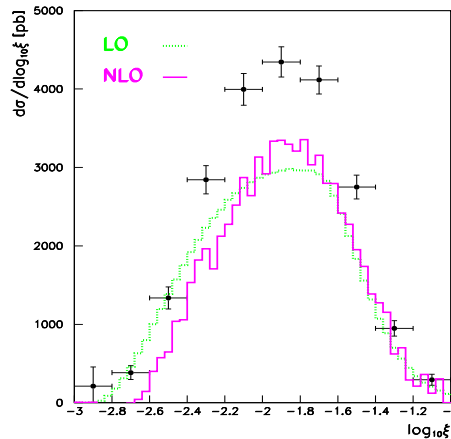


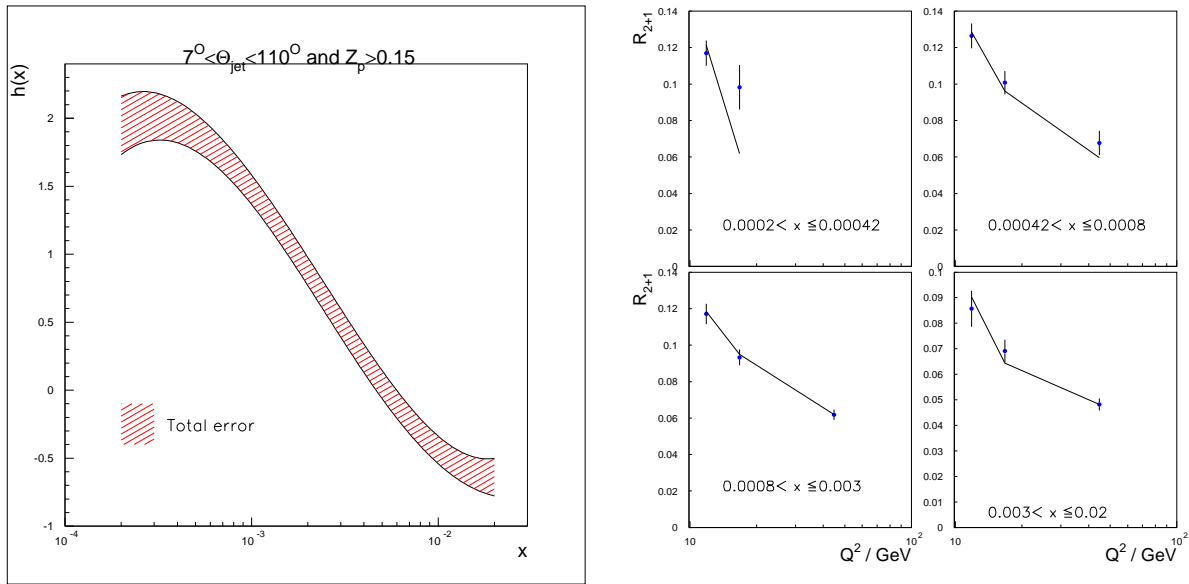
Figure 8: ZEUS preliminary dijet cross section as a function of ξ , compared to LO and NLO predictions.

This is illustrated in Fig. 8 where the ZEUS preliminary dijet cross section, corrected to parton level, is compared to the NLO and LO predictions [34]. The cross section is measured as a function of $\xi = x(1 + M_{JJ}/Q^2)$, the momentum fraction of the parton entering the hard scattering process. The data are $\simeq 30\%$ higher than the NLO calculation and this difference persists after taking into account variations in calorimeter energy scale, jet energy resolution, the Monte Carlo used to correct to parton level, the input parton densities or the factorisation/renormalisation scale. However, the shape of the cross section is well described by the NLO calculations and this can be used to extract the power dependence of the gluon at low- ξ , $\xi g(\xi) \propto \xi^{-\lambda}$. This results in a value of $\lambda = 0.38 \pm 0.04 \pm 0.18$ at $Q^2 = 4 \text{ GeV}^2$.

A further development has been taken in the H1 analysis. Using the k_T algorithm in the Breit frame [37], a global fit has been performed of the H1 and NMC DIS cross section measurements as well as the H1 preliminary dijet rates. In order to account for hadronisation effects, an additional power correction term is incorporated

¹⁾ A similar excess is observed in the ZEUS “resolved” photoproduction dijet data when compared to the NLO calculations for the lowest $E_T > 6 \text{ GeV}$ and relatively low x_γ ($0.3 < x_\gamma^{OBS} < 0.7$) data (see Fig. 2 in [41]).

into the fit of the dijet rates. Although the functional form of these power corrections has not yet been calculated, it is clear from the fits to the data that such a term is required. An empirical function $h(x) = \alpha + \beta \ln(x/x_o) + \gamma \ln^2(x/x_o) + \delta \ln^3(x/x_o)$ is introduced, where α, β, γ and δ are additional parameters in the fit and $x_o = 10^{-4}$. The additional contribution to the dijet cross section is determined as $\Delta\sigma(x, Q^2) = h(x)/Q^2$. The fitted form of $h(x)$ is shown in Fig. 9 together with the results of the global fit incorporating this power correction term. A calculation of the power corrections would therefore enable a simultaneous determination of its magnitude and provide further constraints on α_S as well as the parton densities.



(a) $h(x)$ power correction term.

(b) dijet rates compared to the global fit incorporating the $h(x)$ power correction.

Figure 9: Analysis of H1 dijet data.

BFKL-motivated measurements

Recently, much interest has been focused on the small Bjorken- x region, where one would like to distinguish BFKL [42] from the more traditional DGLAP evolution equation [43]. One of the dominant Feynman graphs responsible for parton evolution in DIS is shown in Fig. 10. The x_i denote the momentum fractions (relative to the incoming proton) of the incident virtual partons and p_{Ti} is the transverse momentum of emitted parton i . Such “ladder-type” diagrams with strong ordering in transverse momenta, $Q^2 \simeq p_{Tn}^2 \gg \dots \gg p_T(j)^2$, but only soft ordering for the longitudinal fraction $x_1 > x_2 > \dots > x_n \simeq x$ are the source of the leading $\log Q^2$ contributions which are summed in the DGLAP evolution equation [43]. In the BFKL approximation, transverse momenta are no longer ordered along the ladder while there is a strong ordering in the fractional momentum $x_n \ll x_{n-1} \ll \dots \ll x_1 \simeq x_{jet}$.

BFKL evolution can be enhanced and DGLAP evolution suppressed by studying DIS events which contain an identified jet of longitudinal momentum fraction $x_{jet} = p_z(j)/E_{proton}$ (in the proton direction) which is large compared to Bjorken x [44]. Furthermore, tagging a forward jet with $p_T(j) \simeq Q$ allows little room for DGLAP evolution while the condition $x_{jet} \gg x$ leaves BFKL evolution active. Assuming BFKL dynamics leads to an enhancement of the forward jet production cross section proportional to $(x_{jet}/x)^{\alpha_P - 1}$, where α_P is the BFKL pomeron intercept, compared to the $\mathcal{O}(\alpha_S^2)$ QCD calculation with DGLAP evolution [46].

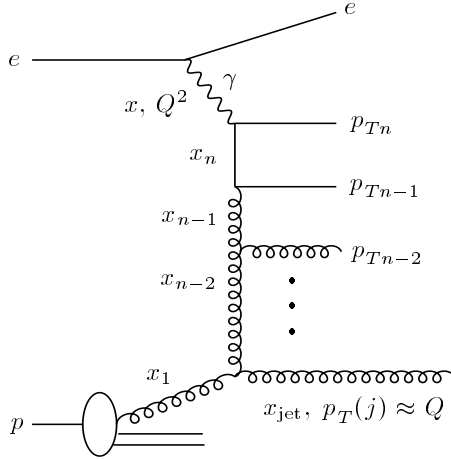


Figure 10: Gluon ladder diagram contributing to jet production in DIS. The position and kinematics of the parton which can give rise to the forward jet is indicated.

In Fig. 11, recent data from H1 [47] and ZEUS [48] are compared with BFKL predictions [49] and fixed order QCD predictions as calculated with the MEPJET [32] program at NLO. The conditions $p_T(j) \simeq Q$ and $x_{jet} \gg x$ are satisfied in the two experiments by slightly different selection cuts. H1 selects events with a forward jet of $p_T(j) > 3.5$ GeV (in the angular region $7^\circ < \theta(j) < 20^\circ$) with

$$0.5 < p_T(j)^2/Q^2 < 2, \quad x_{jet} \simeq E_{jet}/E_{proton} > 0.035; \quad (1)$$

while ZEUS triggers on somewhat harder jets of $p_T(j) > 5$ GeV and $\eta(j) < 2.4$ with

$$0.5 < p_T(j)^2/Q^2 < 4, \quad x_{jet} = p_z(j)/E_{proton} > 0.035. \quad (2)$$

Clearly, both experiments observe substantially more forward jet events than expected from NLO QCD. A very rough estimate of the uncertainty of the NLO calculation is provided by the two dotted lines, which correspond to variations by a factor 10 of the renormalisation and factorisation scales μ_R^2 and μ_F^2 . A recent BFKL calculation (dashed lines) agrees better with the data, but here the overall normalisation is uncertain and the agreement may be fortuitous. Also, we recall that both experiments observe more centrally produced dijet events than predicted by the NLO QCD calculations. Whatever mechanism is responsible for the enhancement in central jet production may also play a role in the enhanced forward jet cross section. Clearly these issues must be resolved before the evidence for BFKL dynamics can be elevated to the status of discovery.

The multiple gluon emission in ladder-type diagrams is also studied in jet-jet decorrelations at the Tevatron. D0 presented preliminary results as a function of the pseudorapidity separation of the two leading jets in an event [50]. The measurement is compared to HERWIG and PYTHIA [5] parton-shower Monte Carlo simulations, and to BFKL predictions. The soft gluon emissions are expected to decorrelate the transverse energy (E_T) and azimuthal angle (ϕ) of the produced jets as the rapidity interval between them increases. HERWIG and PYTHIA simulations reproduce the observed decorrelation reasonably well. However, the leading-log BFKL resummation [51] predicts a larger decorrelation while a NLO QCD calculation underestimates the decorrelation effects. Therefore, no clear conclusion on the question of BFKL dynamics can be drawn from the present Tevatron data.

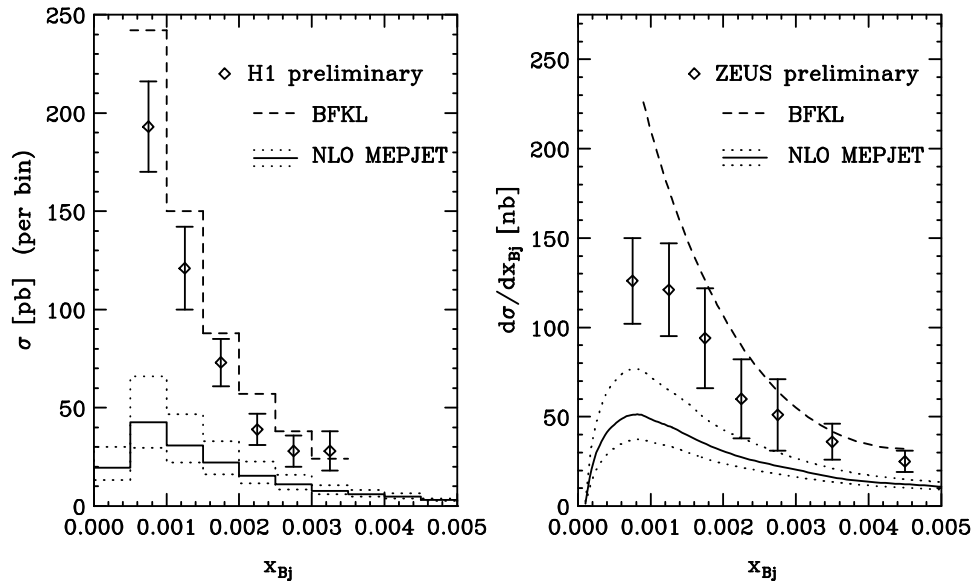


Figure 11: Forward jet cross section at HERA as a function of Bjorken x within (a) the H1 [47] and (b) the ZEUS [48] acceptance cuts. The BFKL result of Bartels et al. [49] is shown as the dashed line. The solid and dotted lines give the NLO MEPJET result for the scale choice $\mu_R^2 = \mu_F^2 = \xi(0.5 \sum k_T)^2$ with $\xi = 0.1, 1$ and 10 , which provides a measure for the uncertainty of the NLO prediction.

Instantons at HERA

Perturbative QCD successfully describes hard scattering processes. Beyond these, nonperturbative processes are predicted by QCD as well, e.g. processes mediated via instanton configurations in the path integral [52]. Of particular interest in ep collisions are instanton processes which simultaneously produce n_f light $\overline{q}_L q_R$ pairs and hence violate chirality by $\Delta Q_5 = 2n_f$ units. Ordinarily these processes are exponentially suppressed, by a factor $\exp[-4\pi/\alpha_S]$. In conjunction with multiple gluon emission, however, this suppression is ameliorated by a factor $\exp[-4\pi F(x')/\alpha_S(\mu)]$, where the so-called “holy-grail function” $F(x')$ equals unity at $x' = 1$. $F(x')$ is known to decrease with decreasing x' , to about $1/2$ at $x' \simeq 0.2$ but is not reliably calculable for small values of x' [52].

The expected fraction, $f^{(I)}$, of instanton induced events, compared to generic DIS events at the same x and Q^2 , depends critically on the shape of the holy-grail function at small x' . Expectations range between $10^{-6} < f^{(I)} < 10^{-3}$ if $F(x')$ approaches a constant below $x'_{min} = 0.2 \dots 0.3$ [52]. Because several $q\overline{q}$ pairs and gluons are produced isotropically, the striking signature of instanton-induced events would be very high particle multiplicity and high average transverse energy deposition over a large region of the available phase space.

H1 reported on a search for such events [53]. The best limits are obtained from the non-observation of events with large charged particle multiplicities. For $80 < W < 220$ GeV, limits of $f^{(I)} \lesssim 0.5\%$ have been set [53]. These limits are still about one order of magnitude larger than expectations from instanton calculations [52], but they begin to probe the interesting parameter range.

W + Jets Production

Hadronic production of W and Z bosons provides a clean probe of perturbative QCD calculations. Three analyses were presented from the $D\bar{O}$ and CDF collaborations utilising the large sample of $p\bar{p}$ collisions accumulated from the 1994-1995 Tevatron Collider run [54].

The first analysis from the CDF collaboration was a measurement of the $W/Z + \geq n$ Jets cross sections for $n = 1 - 4$. Figure 12(a) shows the inclusive associated jet multiplicity distribution for W and Z bosons. The uncorrected data are compared to the CDF detector simulation incorporating the VECBOS [55] LO QCD calculation plus HERWIG [6] parton shower and hadronisation. The CTEQ3M [30] parton densities were used. The band in the theoretical predictions represents the effect of varying the renormalisation and factorisation scales from $Q^2 = M^2 + p_T^2$ of the boson to the $\langle p_T \rangle^2$ of the partons. Using the hard scale, $M^2 + p_T^2$, the LO QCD predictions are about a factor 1.7 lower than the data, for all jet multiplicities. On the other hand the predictions for the softer scale, $\langle p_T \rangle^2$, are in better agreement with the data.

The $D\bar{O}$ collaboration reported results on the ratio of the production cross sections for $W + 1$ Jet to $W + 0$ Jets, \mathcal{R}^{10} , as a function of the minimum jet transverse energy, shown in Fig. 12(b). The data between 20 and 60 GeV are consistently higher than the DYRAD NLO predictions by about a factor of two. This is a rather curious result since it is in a domain where one generally expects QCD to work well.

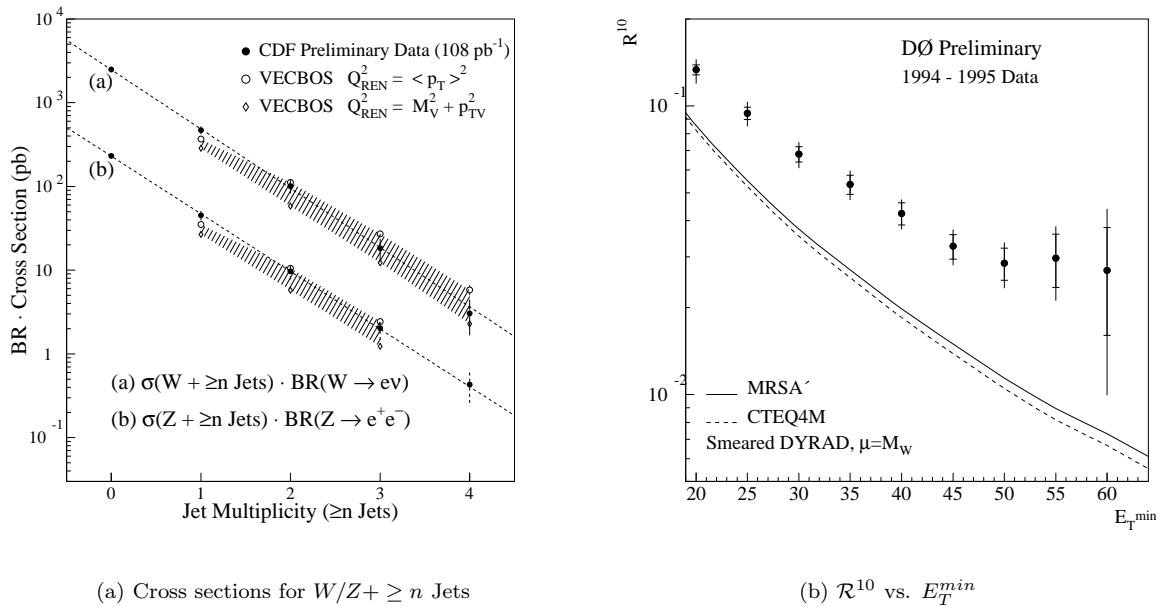


Figure 12: CDF and $D\bar{O}$ results for $W/Z +$ Jets production.

$D\bar{O}$ also investigated color coherence effects in $W +$ Jets events. For this study events with a W boson and opposing jet were selected and the distribution of soft particles around the colorless W boson and the jet (colored parton) was measured. The color coherence signal is observed by comparing the multiplicity distributions of calorimeter towers with $E_T > 250$ MeV around the W and around the jet. It is concluded that both angular ordering and string fragmentation are needed in PYTHIA [5] to describe the data.

Conclusions

The development of NLO calculations for a wide range of hadronic final state variables and the increasingly precise data from HERA, the Tevatron and LEP has provided a detailed testing ground for the strong interaction. At the DIS97 workshop, beautiful agreement of the data from LEP II with QCD was presented. At HERA and the Tevatron various chinks in the armour of QCD were identified. The detailed comparison of these data with the latest developments in the theoretical framework will determine whether the established paradigms are sufficient to understand the many facets of hadronic final state production reported at this workshop.

Acknowledgements

It is a pleasure to thank all the speakers who contributed to the various sessions, as well as those who contributed to the lively discussions following these talks. The success of this working group was in large part due to the outstanding organisation of the workshop by J. Repond and his team.

References

- [1] Yu. L. Dokshitzer and S. I. Troyan, Proc. 19th Winter School of the LNPI, Vol. 1, p.144; Leningrad preprint LNPI-922 (1984); Ya. I. Azimov, Yu. L. Dokshitzer, V. A. Khoze and S. I. Troyan, Z. Phys. **C27** (1985) 65 and **C31** (1986) 213.
- [2] Yu.L. Dokshitzer, V.A. Khoze, A.H. Mueller and S.I. Troyan, *Basics of Perturbative QCD*, Editions Frontières, 1992.
- [3] V.A. Khoze and W. Ochs, preprint MPI-PhT/96-29, Durham DTP/96/36 [hep-ph/9701421]; S. Lupia and W. Ochs, MPI-PhT/97-26 [hep-ph/9704319].
- [4] R.J. Hemingway, these proceedings (and references therein).
- [5] T.Sjöstrand, Comp. Phys. Comm. **82** (1994) 74.
- [6] G. Marchesini et al., Comp. Phys. Comm. **67** (1992) 465.
- [7] L3 Collaboration, M. Accirari et al., Phys. Lett. **B371** (1996) 126.
- [8] Ya. I. Azimov, Yu. L. Dokshitzer and V. A. Khoze, Sov. Phys. Uspekhi, **23** (1980) 732; C. Peterson and T. F. Walsh, Phys. Lett. **91B** (1980) 455; I. Montvay, Phys. Lett. **84B** (1979) 331.
- [9] T.Sjöstrand, Proc. Int. Europhysics Conf. on High Energy Physics, Brussels, Eds. L. Lemonne, C. Vander Velde, F. Verbeure (World Scientific, Singapore, 1996) p. 572.
- [10] F. E. Close, Yu. L. Dokshitzer, V. N. Gribov, V. A. Khoze and M. G. Ryskin, Phys. Lett. **319B** (1993) 291.
- [11] DELPHI Collaboration, CERN-PPE/95-039.
- [12] ZEUS Collaboration, M. Derrick et al., Z. Phys. **C68** (1995) 29; H1 Collaboration, S. Aid et al., Nucl. Phys. **B480** (1996) 3; H1 Collaboration, C. Adloff et al., DESY-97-095, subm. to Z. Phys. C.
- [13] D. Amati and G. Veneziano, Phys. Lett. **83B** (1979) 87; A. Bassetto, M. Ciafaloni and G. Marchesini, Phys. Lett. **B83** (1979) 207; G. Marchesini, L. Trentadue and G. Veneziano, Nucl. Phys. **B181** (1981) 335.
- [14] A. De Roeck, these proceedings (and references therein).
- [15] J. Bromley, these proceedings (and references therein).

- [16] A. Beretvas, these proceedings (and references therein).
- [17] V.A. Khoze, S. Lupia and W. Ochs, preprint MPI-PhT/96-92, Durham DTP/96/90 [hep-ph/9610204].
- [18] S. Lupia and W. Ochs, Phys. Lett. **B365** (1996) 339.
- [19] D. Graudenz, CERN-TH/96-52.
- [20] S. Behrends and J. Lamoreux, these proceedings (and references therein).
- [21] S. Martí i García, these proceedings (and references therein).
- [22] M. Dasgupta, these proceedings (and references therein).
- [23] K. Rabbertz, these proceedings (and references therein).
- [24] M. Martinez, these proceedings (and references therein).
- [25] M. Klasen and G. Kramer, DESY preprint 97-002.
- [26] D.A. Kosower, these proceedings (and references therein).
- [27] B. Hirosky, these proceedings (and references therein).
- [28] F. Chlebana, these proceedings (and references therein).
- [29] S. Ellis, Z. Kunszt, and D. Soper, Phys. Rev. Lett. **64** (1990) 2121.
- [30] CTEQ Collaboration, H.L. Lai et al., Phys. Rev. D **51** (1995) 4763.
- [31] W. T. Giele, E. W. N. Glover and D. A. Kosower, Nucl. Phys. **B403** (1993) 633; Phys. Rev. Lett. **73** (1994) 2019.
- [32] E. Mirkes and D. Zeppenfeld, Phys. Lett. **B380** (1996) 205 [hep-ph/9511448].
- [33] S. Catani and M. H. Seymour, CERN-TH/96-240.
- [34] D. Mikunas, these proceedings (and references therein).
- [35] M. Wobisch, these proceedings (and references therein).
- [36] M. Weber, these proceedings (and references therein).
- [37] F. Zomer, these proceedings (and references therein).
- [38] L. Lönnblad, Comp. Phys. Comm. **71** (1992) 15.
- [39] G. Ingelman, Proceedings of the 1991 Workshop on Physics at HERA, DESY Vol. 3 (1992) 1366.
- [40] H. Kharraziha, these proceedings (and references therein).
- [41] R. Saunders, these proceedings (and references therein).
- [42] E.A. Kuraev, L.N. Lipatov and V.S. Fadin, Sov. Phys. **JETP** **45** (1977) 199; Y.Y. Balitsky and L.N. Lipatov, Sov. J. Nucl. Phys. **28** (1978) 282.
- [43] G. Altarelli and G. Parisi, Nucl. Phys. **126** (1977) 297; V.N. Gribov and L.N. Lipatov, Sov. J. Nucl. Phys. **15** (1972) 438 and 675; Yu. L. Dokshitzer, Sov. Phys. **JETP** **46** (1977) 641.
- [44] A.H. Mueller, Nucl. Phys. B (Proc. Suppl.) **18C** (1990) 125; J. Phys. **G17** (1991) 1443; J. Kwiecinski, A.D. Martin and P.J. Sutton, Phys. Rev. **D46** (1992) 921; W.K. Tang, Phys. Lett. **B278** (1992) 363.
- [45] J. Bartels, A. De Roeck and M. Loewe, Z. Phys. **C54** (1992) 635.
- [46] E. Mirkes and D. Zeppenfeld, Phys. Rev. Lett. **78** (1997) 428 [hep-ph/9609231].

- [47] M. Wobisch, these proceedings (and references therein).
- [48] S. Wölflé, these proceedings (and references therein).
- [49] J. Bartels et al., Phys. Lett. **B384** (1996) 300 [hep-ph/9604272].
- [50] S.Y. Jun, these proceedings (and references therein).
- [51] V. Del Duca and C. Schmidt, Phys. Rev. **D49** (1994) 4510 [hep-ph/9311290] and Phys. Rev. **D51** (1995) 2150 [hep-ph/9407359].
- [52] S. Moch, A. Ringwald and F. Schrempp, these proceedings (and references therein).
- [53] T. Carli, these proceedings (and references therein).
- [54] T. Joffe-Minor, these proceedings (and references therein).
- [55] F.A. Berends et al., Nucl. Phys. **B357** (1991) 32.
- [56] W. T. Giele, E. W. N. Glover, and D. A. Kosower, Nucl. Phys. **B403** (1993) 633.